J Neurophysiol 97: 1588–1599, 2007.
First published November 1, 2006; doi:10.1152/jn.00206.2006.

Encoding of Movement Dynamics by Purkinje Cell Simple Spike Activity During Fast Arm Movements Under Resistive and Assistive Force Fields

Kenji Yamamoto,[1] Mitsuo Kawato,[2] Shinya Kotosaka,[3] and Shigeru Kitazawa[1,4]

[1]*Neuroscience Research Institute, National Institute of Advanced Industrial Science and Technology, Ibaraki;* [2]*ATR Computational Neuroscience Laboratories, Kyoto;* [3]*Saitama University, Faculty of Engineering, Saitama; and* [4]*Juntendo University, School of Medicine, Tokyo, Japan*

Submitted 26 February 2006; accepted in final form 27 October 2006

Yamamoto K, Kawato M, Kotosaka S, Kitazawa S. Encoding of movement dynamics by Purkinje cell simple spike activity during fast arm movements under resistive and assistive force fields. *J Neurophysiol* 97: 1588–1599, 2007. First published November 1, 2006; doi:10.1152/jn.00206.2006. It is controversial whether simple-spike activity of cerebellar Purkinje cells during arm movements encodes movement kinematics like velocity or dynamics like muscle activities. To examine this issue, we trained monkeys to flex or extend the elbow by 45° in 400 ms under resistive and assistive force fields but without altering kinematics. During the task movements after training, simple-spike discharges were recorded in the intermediate part of the cerebellum in lobules V–VI, and electromyographic activity was recorded from arm muscles. Velocity profiles (kinematics) in the two force fields were almost identical to each other, whereas not only the electromyographic activities (dynamics) but also simple-spike activities in many Purkinje cells differed distinctly depending on the type of force field. Simple-spike activities encoded much larger mutual information with the type of force field than that with the residual small difference in the height of peak velocity. The difference in simple-spike activities averaged over the recorded Purkinje-cells increased ~40 ms before the appearance of the difference in electromyographic activities between the two force fields, suggesting that the difference of simple-spike activities could be the origin of the difference of muscle activities. Simple-spike activity of many Purkinje cells correlated with electromyographic activity with a lead of ~80 ms, and these neurons had little overlap with another group of neurons the simple-spike activity of which correlated with velocity profiles. These results show that simple-spike activity of at least a group of Purkinje cells in the intermediate part of cerebellar lobules V–VI encodes movement dynamics.

INTRODUCTION

Simple-spike (SS) activity of Purkinje cells, especially those in the cerebellar hemisphere of lobules IV–VI, has been reported to be modulated during reaching arm movements (Coltz et al. 1999; Fortier et al. 1989; Fu et al. 1997; Liu et al. 2003) and wrist movements (Gilbert and Thach 1977; Mano and Yamamoto 1980; Smith and Bourbonnais 1981; Thach 1968, 1970). However, it is controversial whether the SSs encode movement kinematics, such as the position, direction, and the velocity of movements, or movement dynamics like muscle activities and joint forces. During wrist movements, for example, Gilbert and Thach (1977) suggested that SS activity encodes movement dynamics, but Mano and Yamamoto (1980) reported that the SS activity correlated with the movement speed. Smith and Bourbonnais (1981) suggested that SS activity encodes movement dynamics during precision grips.

In more recent studies, however, no study has supported cerebellar SS coding of movement dynamics in arm reaching movements. Fortier et al. (1989) reported that the SS activity in a population of Purkinje cells collectively encoded movement direction during eight directional two joint arm movements. Ebner and his colleagues (Coltz et al. 1999, 2000; Fu et al. 1997) showed in eight directional visuomotor arm tracking movements that the SS discharge encodes movement velocity in addition to the hand position. The lack of evidence for movement dynamics in arm reaching movements is remarkable because it is often hypothesized in theoretical studies that the SS activity in the cerebellum represents inverse dynamics of arm movements (Kawato 1999; Kawato and Gomi 1992; Wolpert and Kawato 1998), and the SS activity in the cerebellum represents dynamic components of motor commands in ocular following eye movements (Gomi et al. 1998; Kawano 1999; Shidara et al. 1993; Yamamoto et al. 2002c).

Why is there no report about the association between cerebellar activity and movement dynamics during arm movements? A possible reason is that reaching movements involved movements around proximal joints of the elbow and the shoulder, which have not been examined in the previous studies that reported encoding of movement dynamics by SS activity (Gilbert and Thach 1977; Smith and Bourbonnais 1981). Another more plausible reason is that many studies during arm movements were not free from the correlation between movement kinematics and dynamics. Without removing this correlation, the relationship of neural activity with movement dynamics cannot be distinguished from its relationship with movement kinematics and vice versa (Todorov 2000). To see whether the movement dynamics in arm movements is represented in the cerebellum, it is essential to remove the correlation between movement kinematics and dynamics.

For this purpose, we trained monkeys to flex or extend their elbows by 45° in 400 ms under distinctly different force fields but without altering the movement kinematics. We used a resistive viscous force field and another negative viscous force field that assisted movements in proportion to the angular velocity of the elbow joint (Krouchev and Kalaska 2003; Wada et al. 2003; Yamamoto et al. 2000). After the animals were trained to achieve almost identical velocity profiles under the two force fields, we recorded SS activities from Purkinje cells

Present address and address for reprint requests and other correspondence: K. Yamamoto, University of Pittsburgh, Department of Neurobiology, 4074 Biomedical Science Tower 3, 3501 Fifth Ave., Pittsburgh, PA 15261 (E-mail: kenjiy@pitt.edu).

The costs of publication of this article were defrayed in part by the payment of page charges. The article must therefore be hereby marked "*advertisement*" in accordance with 18 U.S.C. Section 1734 solely to indicate this fact.

in the intermediate part of lobules IV–VI. We focused on this part of the cerebellum because the area reportedly has connections with the primary motor cortex (Kelly and Strick 2003). Some neurons of primary motor cortex represent the dynamics of arm movements (Evarts 1968; Kakei et al. 1999; Kalaska et al. 1989; Scott and Kalaska 1997; Sergio and Kalaska 1997, 1998).

We here show that the disparity in SS activity of many Purkinje cells between the two force fields correlated with the difference in dynamics but not with the residual small differences in movement kinematics. We also show that the disparity in SS activity between two force fields appeared before the appearance of the difference in electromyographic (EMG) activities. From results of linear regression analysis, we further suggest that there are two groups of Purkinje cells, one representing movement dynamics and the other representing movement kinematics.

Some of the results reported here have been presented previously in abstract form (Yamamoto et al. 2000. 2002a,b).

METHODS

Subjects

Two male monkeys (*Macaca fuscata,* 10-11kg, *monkeys M* and *P*) were used. The experiments were approved by the institutional committees for animal experimentation (National Institute of Advanced Industrial Science and Technology) and followed the *Guiding Principles for the Care and Use of Animals* approved by the Council of the Physiological Society of Japan.

Apparatus and task procedures

Each monkey was seated in a primate chair and placed the right arm on a single-joint manipulandum with a torque motor (Fig. 1). The manipulandum was developed in the Kawato Dynamic Brain Project (ERATO, JST). The same one was used by Krouchev and Kalaska (2003) and a similar one was used by Wada et al. (2003). The forearm and the wrist were fixed in a brace so that the monkey could make elbow flexion and extension movements without moving the wrist. A green cursor (hand position, 0.96° in diameter) and a white circle (target, 2.87°) were displayed on a CRT monitor that was 40 cm in front of the monkey (Fig. 1). The cursor moved on an arc (radius, 20 cm; central angle, 90°) that represented the path of the hand viewed from above.

Each trial began when a target was presented in the midpoint of the arc (0°). The animal was required to place the cursor in the target by adjusting the forearm to a neutral position. After a variable period (1–1.5 s), the target jumped randomly to one of the two ends of the arc (+45 or −45°). The monkey was required to move the cursor to the target by flexing or extending its elbow by 45°. A drop of juice was given to the monkey if it initiated an elbow movement in 600 ms after the jump of the target, moved the cursor into the target circle within a time window between 200 and 400 ms after the movement onset and kept the cursor within the target for 600 ms.

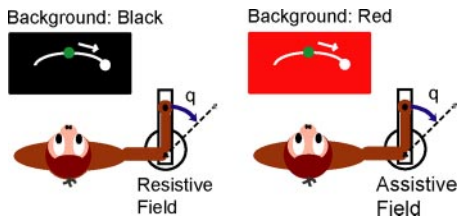

FIG. 1. Apparatus and task procedures. Monkeys placed the right arm on a single-joint manipulandum with a torque motor. A CRT monitor was placed 40 cm in front of the monkey and displayed a green cursor (hand position) and a white circle (target). The monkeys were required to move the cursor from the neutral position to the target by flexing or extending the elbow by 45°. During the movement, the torque motor generated a viscous force that was either assistive (red background) or resistive (black background). The 2 force fields were alternated every 10 trials.

During the movement, the torque motor generated a viscous force (τ) that was in proportion to the angular velocity of the elbow joint. The force was defined as

$$\tau = -W\dot{q} \quad (1)$$

in which q denote the angle of the elbow joint (Fig. 1) and W denotes the coefficient of viscosity. In the experiments, we used two coefficients. One positive coefficient (0.25 Nms/rad) generated resistive, and the other negative coefficient (−0.25 Nms/rad) generated assistive force during the movements.

The two force fields were alternated every 10 trials. The number of flexions and extensions in each block of 10 trials fluctuated due to the completely random assignment of the movement direction. The background color on the CRT screen was switched according to the type of force field: it was black when the field was resistive and red when the field was assistive (Fig. 1) so that the monkey could tell which type of force field would be applied in the upcoming movement. Intertrial intervals were randomly variable (1–1.5 s). The animals carried out ~500 trials per day on average.

Training

The animals were initially trained for 30–50 wk without any force field with the black background color on the CRT. After the animals became able to carry out the task movements under the null field, the animals were trained under the assistive force field with the red background for 4–19 wk. Then we started training them under the null (black background) and the assistive (red background) force fields. The two fields were alternated every 12 trials at the beginning and every 10 trials thereafter. The null field was gradually replaced with the resistive force field by increasing the viscous coefficient day by day in 4–6 wk until the monkeys became able to switch between the two force fields.

Surgery

After training, animals were anesthetized with pentobarbital sodium, and a chronic recording chamber and head holder were implanted on the skull. The chamber was placed above lobule V of the cerebellum ipsilateral to the trained arm (right). Coronal and sagittal images of the head and the brain were taken beforehand with a 3T magnetic resonance scanner (GE-Sigma, Milwaukee, WI) to determine the position of implantation for each monkey. EMG electrodes were implanted subcutaneously on the long head of the biceps muscle of *monkey M* and on the long head of the biceps and the middle head of the triceps muscles of *monkey P.* Leads were passed through subcutaneous tunnels from each muscle to the site of a connector implanted on the monkey's back (Miller et al. 1993).

Electrophysiology

The SS and complex spike discharges of cerebellar Purkinje cells were recorded extracellularly using high-impedance, glass-coated tungsten microelectrodes. Signals were amplified, digitized at 30 kHz, wave-form discriminated with a PC-based spike discriminator that applies a principal-component analysis to each spike form and converted to pulses before storage to computer at 2 kHz. Amplified signals were continuously recorded with a bandwidth of 10 kHz in a digital data recorder (TEAC, RD-125T) as a backup. Signals were continuously monitored through headphones and on an oscilloscope, and each discriminated spike form

was monitored on the PC display and two additional oscilloscopes. Purkinje cells were identified by the presence of spontaneous complex-spike discharge (Fig. 2*B*). The activities of 93 and 98 Purkinje cells were recorded from *monkeys M* and *P,* respectively. Of them, 62 and 34 yielded enough data for further analysis in that their SS discharges were recorded for >18 trials for both flexion and extension under each force field. To further confirm that the discharges were recorded from Purkinje cells, we calculated coefficients of variation of interspike intervals during a premovement period (−350 to −200 ms). Coefficients of variation ranged from 0.58 to 1.14 (mean, 0.80) in *monkey M* and 0.58 to 1.03 (mean, 0.78) in *monkey P*. These values were larger than those reported for granular layer units including presumed Golgi cells (0.04 to 0.37) (Miles et al. 1980). Figure 2 *B, C,* and *D* exemplifies raw spike data recorded from a Purkinje cell (*monkey M*) and raster plots of SS and complex-spike discharges of the same Purkinje cell. We recorded from all Purkinje cells that were encountered, irrespective of their discharge characteristics.

The EMG signals were recorded from the biceps and triceps muscles at 2 kHz simultaneously at the time of neural recording. The EMG of triceps of *monkey M* was recorded with a surface EMG electrode.

Histology

At the conclusion of recordings in the monkeys, electrolytic lesions were made by passing DC (10 μA for 40 s) through the tip of the recording microelectrode. The animals were killed with pentobarbital and perfused through the heart with saline followed by 10% Formalin. The animal's brain was removed, and frozen sections were cut at 50 μm in the sagittal plane, mounted on microscope slides, and stained with cresyl violet for cell bodies.

Using the lesions as a reference, recording sites were reconstructed from the serial sections. The recording areas are shown in Fig. 2*A* relative to a dorsal view of the cerebellar cortex. In both animals, the loci of the recordings were either anterior to the primary fissure in lobule V or posterior in lobule VI. In *animal M* (closed circles), the recordings were centered ~7.5 mm to the right of the midline, and in *animal P* (open circles), they were centered 11 mm to the right of the midline. These recording sites overlapped with the area that was reported to be interconnected with the arm area in the primary motor cortex (Kelly and Strick 2003).

Data analysis

Stored data were analyzed off-line using MATLAB. The position (angle) signal of the manipulandum, measured by a high-resolution

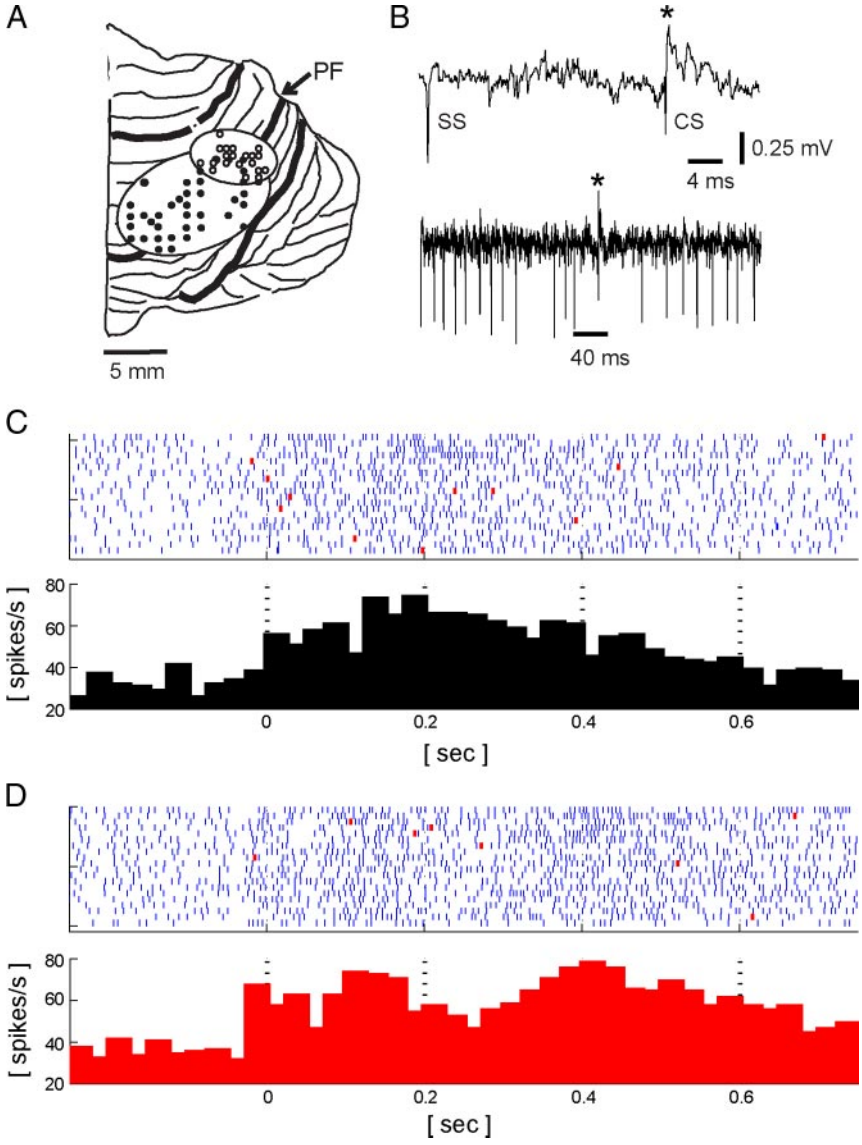

FIG. 2. *A*: areas of recording. Penetration tracks in 2 monkeys (*M* and *P*) are shown relative to a dorsal view of the cerebellar cortex. In both animals, the loci of the recordings were either anterior to the primary fissure (PF) in lobule V or posterior in lobule VI. In *animal M* (closed circles), the recordings were centered ~7.5 mm to the right of the midline, and in *animal P* (open circles), they were centered 11 mm to the right of the midline. *B*: simple (SS)- and complex-spike activity (CS) recorded from a Purkinje cell (*monkey M*). *Top*: part of activity in the lower trace marked by a horizontal bar (40 ms). CS activity is marked (*) in both traces. *C* and *D, top*: raster plots of simple spikes (bars) and complex spikes (red squares) recorded from the same Purkinje cell under resistive (*C*) and assistive (*D*) force field. *Bottom*: average discharge frequencies. Plots are aligned at the movement onset (*time 0*). Bin width is 25 ms.

encoder and recorded at 2 kHz simultaneously at the time of neural recording, was digitally differentiated to obtain velocity and acceleration that were filtered with a two-pole, 100-Hz low-pass Butterworth filter. EMG data were full-wave rectified and were filtered with a two-pole, 100-Hz high-pass Butterworth filter. The neural activities, movement velocities, and EMGs were aligned to the onset of arm movement that was defined as the time when both the movement speed and the acceleration exceeded thresholds of 6°/s and 200°/s^2.

Information analysis

To quantify the differences in velocity, EMG activity, and SSs under the assistive and resistive force fields, we calculated the mutual information between the type of force field and each parameter (velocity, EMG and SS). We calculated the information values in a given 50-ms time window (e.g., shaded area in Fig. 5*A*) and repeated the calculation as we moved the time window along the entire time course of elbow flexion and extension in steps of 0.5 ms. In each time window, we assigned four parameters to every trial: the angular velocity, the EMG signals for the biceps and triceps, and the count of SS within the 50-ms time window. To calculate the mutual information between one of the parameters and the type of force field, we divided all trials during recordings from each cell into a 2 × 2 contingency table according to whether the parameter was greater than or equal to the median or smaller than the median and whether the type of force field was resistive or assistive (Table 1). If the *i*th row and *j*th column of the 2 × 2 cell counts are n_{ij}, the mutual information I was calculated as

$$I = \sum_{j=1}^{2} ((n_{1j} + n_{2j})/N)(H - H_j) \quad (1)$$

in which H, H_j, and N are defined as follows

$$H = -\sum_{i=1}^{2} ((n_{i1} + n_{i2})/N) \log_2((n_{i1} + n_{i2})/N)$$

$$H_j = -\sum_{i=1}^{2} (n_{ij}/(n_{1j} + n_{2j})) \log_2(n_{ij}/(n_{1j} + n_{2j}))$$

$$N = n_{11} + n_{12} + n_{21} + n_{22}$$

If the 2 × 2 cell counts in the table were not significantly different from the cell counts expected from the marginal distribution (χ^2 test, $\alpha = 0.05$), we judged that there was no mutual information and assigned a zero value (Kitazawa et al. 1998). We further defined the information transmission rate I_r as $I_r = I/w$ where w denotes the width of the time window (0.05 s). We assigned I_r to the midpoint of each time window.

TABLE 1. *Mutual force field and simple-spike activity information*

	Numbers of Trials		
Force Field	No. of Spikes ≥Median	<Median	Summation
Resistive field	16 (24)	21 (13)	37
Assistive field	31 (23)	3 (11)	34
Summation	47	24	71

Contingency table for calculating mutual information between the force field (resistive or assistive) and simple-spike activity shown in Fig. 5*A* during shaded area (150–200 ms after movement onset). Numbers in parentheses are the counts expected from the marginal distributions. Median was median of the numbers of simple spikes in the 50-ms time window among the 71 trials.

We additionally calculated the mutual information between each parameter (EMG, SSs) and the peak velocity to test whether these parameters encode kinematics (velocity) of the arm movements. For this purpose, instead of the type of force field, trials for each Purkinje cell were divided into two groups according to whether the peak velocity was larger than or equal to the median or smaller than the median of the peak velocity.

Comparison of latencies in SS and EMG modulations

To examine whether the onset of modulation of SS activities led or lagged that of the EMG modulations on average, we rectified the modulation of SS activity from the baseline firing rate in the following manner

$$g(t) = |f(t) - f_{const}| \quad (2)$$

where $f(t)$ is the temporal firing rate of each Purkinje cell at time t and f_{const} is the average of $f(t)$ over a premovement period from 200 to 100 ms before the movement onset. $f(t)$ was estimated for each Purkinje cell by smoothing the raw spike count histogram (0.5-ms bin) with a Gaussian filter (SD = 25 ms). The rectified modulation of SSs [$g(t)$] was calculated for each trial and averaged over all trials and then over all Purkinje cells in the two monkeys [$G(t)$]. The onset of modulation was defined as the time when $G(t)$ increased by 2 SD from the control level during the premovement control period.

The EMG activities recorded with the SS activities were rectified for each trial and averaged over all trials for each muscle. The onset of modulation was defined in the same manner as for SS modulation (2 SD).

We also compared the onset of the difference in SSs due to the two force fields with the onset of the difference in EMGs. For this purpose, we subtracted SS activity in the resistive force field [$f_+(t)$] from that in the assistive force field [$f_-(t)$] and rectified the subtraction as

$$h(t) = |f_+(t) - f_-(t)| \quad (3)$$

where $h(t)$ denotes the difference of SS activity due to the different force fields.

The onset of the difference in SS activity due to the different force fields was defined as the time when the averaged $h(t)$ increased by 2 SD from the level during the control period. In the same manner, we defined the onset of the difference in EMG activity due to the difference in force fields.

SS activity in the first trials

We further examined whether the SS activity switches instantaneously in the first trial when the force field was switched from one to the other. For this purpose, we chose two (*monkey M*) and one (*monkey P*) Purkinje cells that showed distinct SS activity under the two force fields. These cells had mean mutual information (SS and force field) >0.25 bits from −200 to 700 ms and had more than six first trials for at both types of switching (resistive to assistive and vice versa). The mean SS activity in the first trials was compared with the SS activity averaged over all trials under the same force field (all trials) and that under the different (preceding) force field, by calculating correlation coefficients.

Linear regression of EMG and velocity by SS activity

Temporal patterns of EMG activities and velocity profiles were reconstructed from single-cell SS activity to see whether the SS activity of each Purkinje cell resembled temporal patterns of the dynamics or those of kinematics of the movements. We reconstructed the temporal patterns (between −200 ms and 600 ms from the movement onset) from the SSs recorded from each Purkinje cells as follows

$$m_k(t) = w_{ik} \cdot f_i(t + d_m) + \text{bias} \quad (4)$$

$$v(t) = w_i \cdot f_i(t + d_v) + \text{bias} \quad (5)$$

in which $m_k(t)$, $v(t)$, $f_i(t)$, w_{ik}, w_i, d_m, and d_v denote the EMG activity of the kth muscle at time t, velocity at time t, firing frequency of the ith cell at time t, weighting coefficients of the ith cell on the kth muscle, weighting coefficients of the ith cell on velocity, the time lag from muscle activity to SS activity and the time lag from velocity to SS activity, respectively. Note that a negative time lag indicates that SS activity led muscle activity or velocity in time. Linear regressions were repeated with different time lags d that were changed from −200 to 200 ms with a step of 10 ms. The time lag that yielded the largest determination coefficient (r^2) was chosen as an estimation. A single combination of w_{ik}, d_m, and bias was estimated for each muscle to reconstruct all EMG activities in both flexion and extension under both force fields. Likewise, a single combination of w_i, d_v, and bias was estimated to reconstruct all velocity profiles in both flexion and extension under both force fields.

RESULTS

Velocity and EMG profiles after training

After 4–6 mo of extensive training, the animals were able to flex and extend their elbows under the two distinct force fields without much altering the velocity profiles (kinematics). Figure 3*A* (*top*) shows, for example, that the mean velocity profile under the resistive force field (black curves) was almost identical to that in the assistive force field (red curves) in both flexion (left) and extension (right).

Figure 3*B* (biceps) and *C* (triceps) show the temporal profiles of EMG averaged over trials after extensive training (*monkey M*). It is evident that the EMG profiles of the agonists, the biceps in flexion (Fig. 3*B*, *top left*) and the triceps in extension (Fig. 3*C*, *top right*), were distinctly larger under the resistive force field (black traces) than under the assistive force field (red traces). This difference contrasts clearly with the average velocity profiles that were almost identical under the resistive (black curves in Fig. 3*A*) and assistive (red curves) force fields. Similar results were obtained from *monkey P* (not shown).

It is worth noting that there was little overshoot or undershoot in the peak velocity even in the very first trial when the force field was switched from the resistive to the assistive (red circles in *top panels* of Fig. 4) or from the assistive to the resistive (black circles). Whereas the peak velocity (kinematics) was maintained around a constant level between 200 and 300°/s in both force fields (Fig. 4, *top*), the mean EMG activity that represented movement dynamics alternated between larger and smaller values according to the type of force field. This change occurred at the first trial after the force fields were switched (Fig. 4, *bottom, left*: EMG of the biceps; *right*: EMG of the triceps). That is, the animals were able to switch between the two motor strategies, just by relying on the background color of the monitor (Fig. 1).

SS activity under the two force fields

Figure 5*A* (*top*) exemplifies the mean discharge rate of SSs that were recorded from a Purkinje cell in lobules V–VI (*monkey M*). In flexion (*left*), the mean discharge rate under the resistive force field (37 trials, black trace) was more than twice as large as that under the assistive force field (34 trials, red trace) in the first half of the movement (100–250 ms after the movement onset), showing a distinct difference. To quantify the difference, we calculated the mutual information between the type of force field (assistive or resistive) and the number of SSs during a 50-ms time window (larger or smaller than the median). As an example, let us set a 50-ms time window ranging from 150 to 200 ms after the movement onset (Fig. 5*A*, shaded area). In the 71 trials in which we recorded SS discharges from the Purkinje cell during flexion, 37 and 34 trials were obtained under the resistive and assistive force field, respectively. We divided these 71 trials into two groups according to the number of SSs during the time window. In this

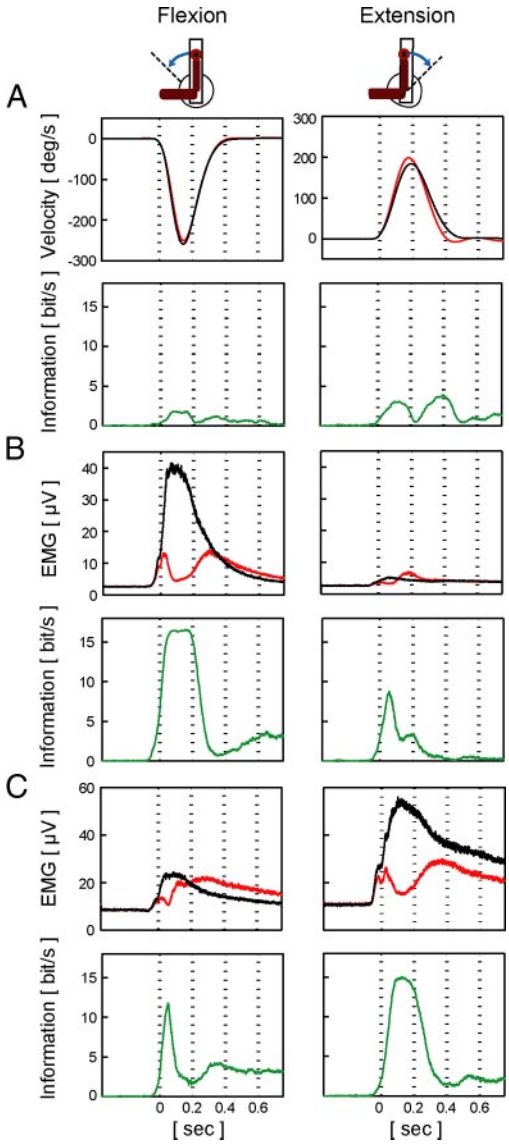

FIG. 3. Mean velocity profiles (*A*) and electromyographic (EMG) activities (*B*: biceps, *C*: triceps) during flexion (*left*) and extension (*right*) in *monkey M*. Black and red traces in *top panels* show data under the resistive and assistive force fields, respectively. Data were initially averaged over trials for each Purkinje cell under each force field (18–88 trials; average 40.2 trials) and then averaged over all Purkinje cells (n = 62). Note almost identical velocity profiles (*A*) in contrast to distinct EMG activities (*B* and *C*). Green traces in *bottom panels* show the mean mutual information between the type of force field and velocity (*A*, *bottom*) and between the type of force field and EMG activities (*B* and *C*, *bottom*). Traces are aligned at the onset of the movement (*time* 0).

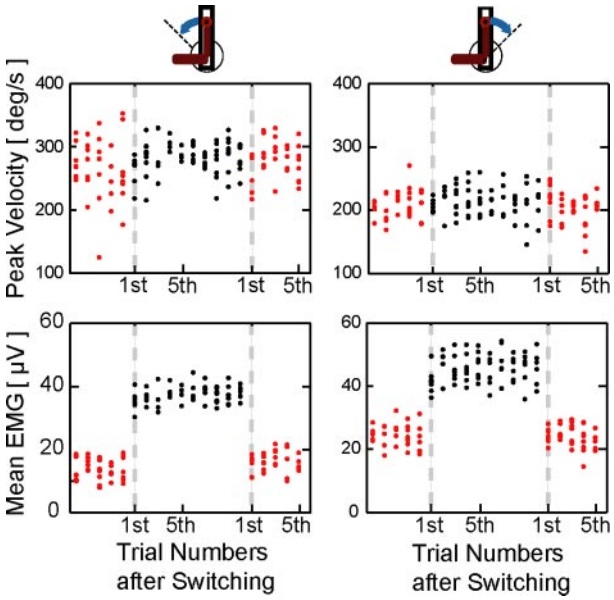

FIG. 4. Instantaneous switching of motor skills after training (*monkey M*). Trial-by-trial peak of absolute value of velocities (ordinate, *top*) and mean EMG activities of agonist muscles (ordinate, *bottom*) are plotted against trial sequence (abscissa) after switching from the assistive (red dots) to the resistive (black dots) force fields and vice versa. Each dot represents 1 trial. Data from 14 blocks of 10 trials under each force field (140 trials) are shown separately for flexions (*left,* EMG of biceps in the *left bottom*) and extensions (*right*, EMG of triceps in the *right bottom*).

case, we divided them into trials with SSs equal to or larger than 3 (spikes/50 ms) and those with SSs equal to or <2 (spikes/50 ms). Thus we categorized the 71 trials in a 2 × 2 factorial manner, as shown in a contingency table (Table 1). The number of trials in each of the four cells [(16, 21; 31, 3)] was significantly different from the counts [(24, 13; 23, 11)] expected from the marginal distributions (χ^2 test, $P < 0.0001$, df = 1, $\chi^2 = 16.2$). To describe more precisely, the two factors were not independent of each other, showing that we can to some extent predict the number of SSs from the type of force field or predict the type of force field from the number of SSs during this 50-ms period. The mutual information thus obtained was 0.20 bits (4.1 bits/s, see METHODS for calculation). The largest possible value of mutual information was 1 bit (1 bit/50 ms = 20 bit/s) when the prediction was perfect, and the smallest was zero when the SS number was independent of the type of force field. By moving the 50-ms time window, we obtained the time course of the mutual information, which provided a good measure of difference in SS discharges according to the type of force field (Fig. 5*A*, *bottom left*). The information plot quantitatively shows that the difference of SSs was evident during the initial half of the movement (100–250 ms). In extension trials, on the other hand, the SS discharge rate in the resistive force field was similar to that in the assistive force field (Fig. 5*A*, *top right*). Accordingly, the information measure was zero for the entire period of premovement and movement periods (Fig. 5*A*, *bottom right*).

We show data from five other Purkinje cells in Fig. 5, *B–F*. The Purkinje cell in Fig. 5*B* showed little difference in flexion but showed distinctive responses in extension, whereas the other four cells (Fig. 5, *C–F*) showed differences in both flexion and extension. The cells in Fig. 5, *C* and *D*, showed a difference prior to the movement onset in extension (*right*). Of the 62 and 34 cells in the monkeys M and *P,* to which we applied the information analysis, 60 and 34 yielded significant information ($P < 0.01$, df = 1, $\chi^2 = 6.63$) during the period between 100 ms before and 600 ms after the movement onset (−100–600 ms). Figure 6 shows the mean information of the 62 cells recorded from *monkey M*. The mean information curve of SS activity reached a peak at ~150–200 ms in both flexion (*left*) and extension (*right*) and decreased thereafter. The shapes of SS information curves (Fig. 6) were similar to those of the agonists (Fig. 3, *B bottom left,* and *C, bottom right*) that reflected a clear difference in the dynamics of movements under the two force fields. These results are consistent with the idea that the SS activity represented the difference in force (dynamics).

However, it may still be argued that the disparity in SS activity did not reflect the difference in the dynamics but reflected smaller differences in the velocity curves (Fig. 3*A*, *top*) however small they might seem. To test this possibility, we evaluated the difference in the velocity curve according to the type of force field using the same information measure. Significant differences in velocity profiles were detected as shown in the information curves (Fig. 3*A*, green traces in the *bottom panels*) that had peaks at ~150 ms from the movement onset. It thus remains possible that the disparity in SS discharge reflected the small difference in kinematics.

To test whether the information measure in SS activity paralleled that in the velocity or that in EMG activity, we divided all trials under both force fields into two groups not by the force field but by the peak velocity (high- and low-velocity groups, Fig. 7*A*, top) and calculated the mutual information between the peak velocity and each parameter. This time, the difference in velocity profiles became larger (Fig. 7*A*, *top*), but the difference in EMG activities became much smaller (Fig. 7, *B* and *C*, *top*) than when the trials were divided according to the type of the force field (Fig. 3). Correspondingly, the information encoded by the velocity profiles became larger (~12 bit/s; Fig. 7*A*, *bottom*), but the information in EMG activities became smaller (Fig. 7, *B* and *C, bottom*) as compared with their counterparts in Fig. 3. As for the information encoded by SS activity, it decreased as shown in Fig. 8 and it correlated with the information encoded by EMG but not with the information encoded by the velocity.

The result shows that the information in SS shown in Fig. 6 was not derived from the small residual difference of movement kinematics but from the large difference of movement dynamics.

Although we have shown that the SS activity reflected movement dynamics, we still do not know whether the SS activity led or lagged the EMG activity. To clarify this point further, we examined whether the onset of modulation in SS activity led or lagged that of EMG activity (Fig. 9, *A* and *C*). The modulation of SS activity crossed a level of significance (2 SD of premovement control period) at −107 ms, but the modulation of EMG crossed the 2 SD level at −64 ms. The results clearly show that the onset of SS modulation led the onset of the increase in muscle activity by ~40 ms.

We also compared the onset of the disparity in SS activities with the onset of the disparity in EMG activities due to the difference in the force fields (Fig. 9, *B* and *D*). SS activity in the resistive force field started to differ from that in the assistive force field 79 ms before the movement onset (−79

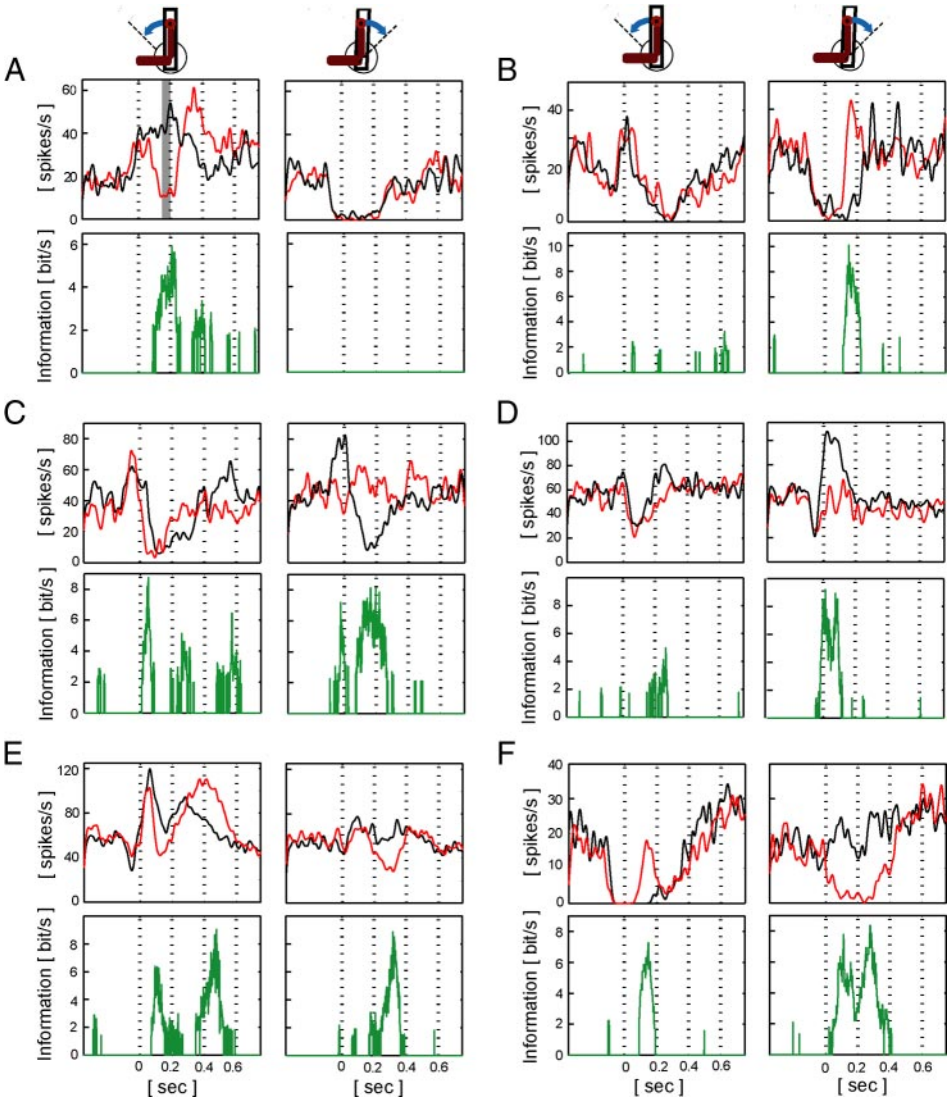

FIG. 5. Temporal patterns of SS activity in single Purkinje cells (*A–D*, 4 cells from *monkey M; E* and *F*, 2 cells from *monkey P*) during flexions (*left*) and extensions (*right*). Black and red traces in *top panels* show the mean discharge rate under the resistive and assistive force fields, respectively. Green traces in bottom panels show the mutual information between the type of force field and SS activity, which is a measure of the difference in simple spike activity due to the difference of force fields. Traces are aligned at the movement onset (*time 0*).

ms, Fig. 9*B*), whereas EMG activities started to differ at −55 ms. Again, the onset of changes in SS activities led the onset of changes in EMG activities. These temporal relationships suggest that the SS activities could be the origin of EMG activities at least in their initial part.

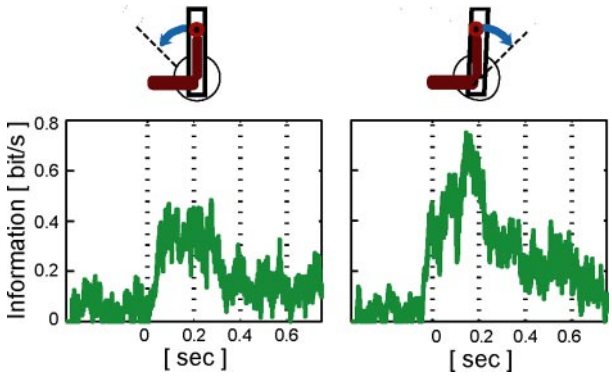

FIG. 6. Temporal patterns of mutual information between the type of force field and simple spike activity. The mutual information was averaged over 62 Purkinje cells (*monkey M*) for flexions (*left*) and extensions (*right*).

SS activity in the first trials

We further examined whether the SS activity switches instantaneously in the first trial when the force field was switched from one to the other. Panels in Fig. 10*A* show example data recorded from a Purkinje cell. Under the resistive force field (*top right*), SS activity showed a gradual decrease before the movement onset, and a further drop and succeeding quick recovery within ~100 ms after the movement onset. Under the assistive force field, on the other hand, the neuron showed a gradual increase before the movement onset, and an abrupt drop and gradual recovery in ~500 ms after the movement onset (*bottom right*). In the first trials after the force field was switched from assistive to resistive force field (*top left*), the time course of SS activity apparently resembled more the activity in the mean resistive force field (*top right,* $r = 0.73$, $P < 0.0001$) than the mean activity in the preceding assistive force field (*bottom right,* $r = 0.17$, $P = 0.43$). Likewise, SS activity in the first assistive trials (*bottom left*) showed a larger correlation with the mean SS activity in the assistive field (*bottom right,* $r = 0.81$, $P < 0.0001$) than with that in the resistive force field (*top right,* $r = 0.35$, $P = 0.10$). In three Purkinje cells that we examined (Fig. 10*B*), SS activity in the

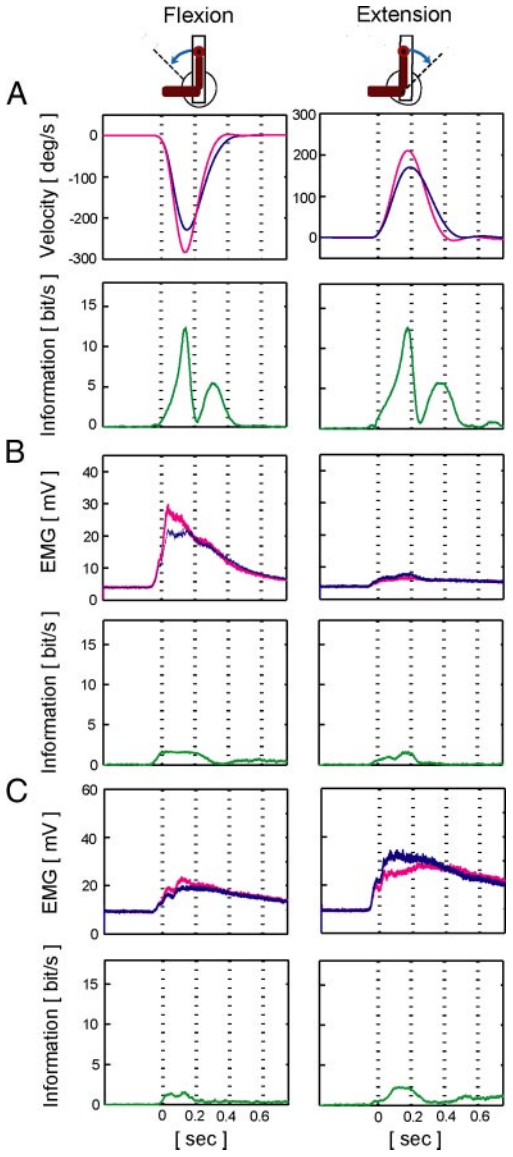

FIG. 7. Mean velocity profiles (*A*) and EMG activities (*B*: biceps, *C*: triceps) during flexion (*left*) and extension (*right*) in *monkey M*. The same data as in Fig. 3 were divided by the peak velocity rather than by the force field. Bright red traces in *top panels* show data in trials with higher peak velocities and blue traces show those with lower peak velocities. Green traces in *bottom panels* show the mutual information between the peak velocity (high/low) and instantaneous velocity (*A, bottom*) and between the peak velocity (high/low) and EMG activities (*B* and *C, bottom*). Traces are aligned at the onset of the movement (*time 0*).

first trials showed significantly greater correlation with the mean SS activity in the same force field (0.69 ± 0.19, mean ± SE) than with the mean SS activity in the preceding force field (0.18 ± 0.21; $P < 0.01$, paired *t*-test). The results suggest that SS activity switches instantaneously from the first trial.

Linear reconstruction of EMGs and velocity profiles from SSs

The results so far suggest that SS activity of at least a group of Purkinje cells in the recorded area encodes movement dynamics. However, it is still possible that SSs of others encode movement kinematics as reported previously (Coltz et al. 1999, 2000; Fortier et al. 1989; Fu et al. 1997). To examine this possibility, we further determined whether SS activity of each neuron had correlation to EMGs or velocity profiles.

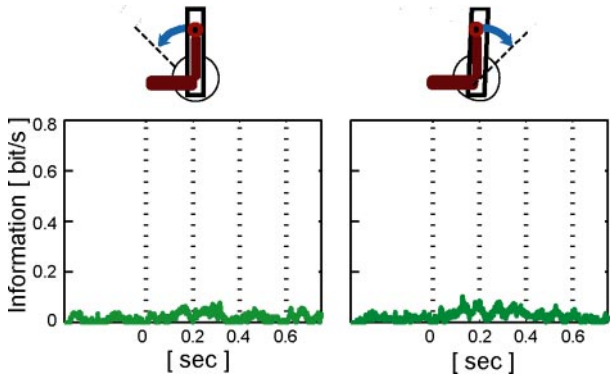

FIG. 8. Temporal patterns of mutual information between peak velocity (high/low) and SS activity. The mutual information was averaged over 62 Purkinje cells (*monkey M*) for flexions (*left*) and extensions (right). Note the smaller information about the peak velocity than that about the force field shown in Fig. 6.

First, EMG activities of each muscle were approximated by the SS firing rate recorded from each single Purkinje cell. A single pair of coefficients (*w*, *d,* and bias in *Eq. 4*) for each muscle was estimated to explain all EMG activities in both flexion and extension under both resistive and assistive force fields. Figure 11*A* shows the distribution of the estimated time lag (*d*) with the mode of −80 ms. Estimated time lags were negative in the majority of Purkinje cells (61 and 70% for biceps and triceps, respectively, muscles in *monkey M;* 75 and 67% for biceps and triceps muscles, respectively, in *monkey P*), suggesting that the modulation in SS activities led the modulation in the EMG profile. The linear regression was

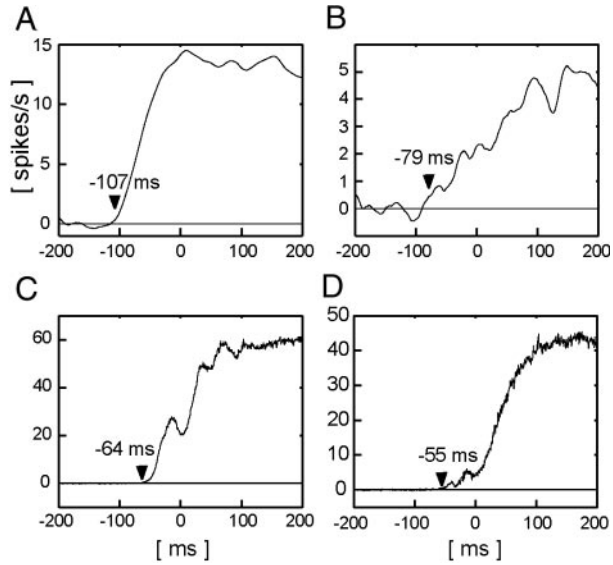

FIG. 9. Modulations in simple spike activities (*A* and *B*) and in EMG activities (*C* and *D*) plotted against the time from the movement onset (abscissa). *A* and *C*: absolute size of modulation relative to the mean activity during a premovement control period (between −200 and −100 ms). *B* and *D*: absolute difference of activities under the 2 force fields. ▲, time at which the modulation exceeded the level of 2 SD during the control period. The data were averaged over all available Purkinje cells (*A* and *B*) and muscles (*C* and *D*) of the two monkeys. Note that the onsets of simple spike modulation (*A*, −107 ms; *B*, −79 ms) led those of EMGs (*C*, −64 ms; *D*, −55 ms) by ~20–40 ms.

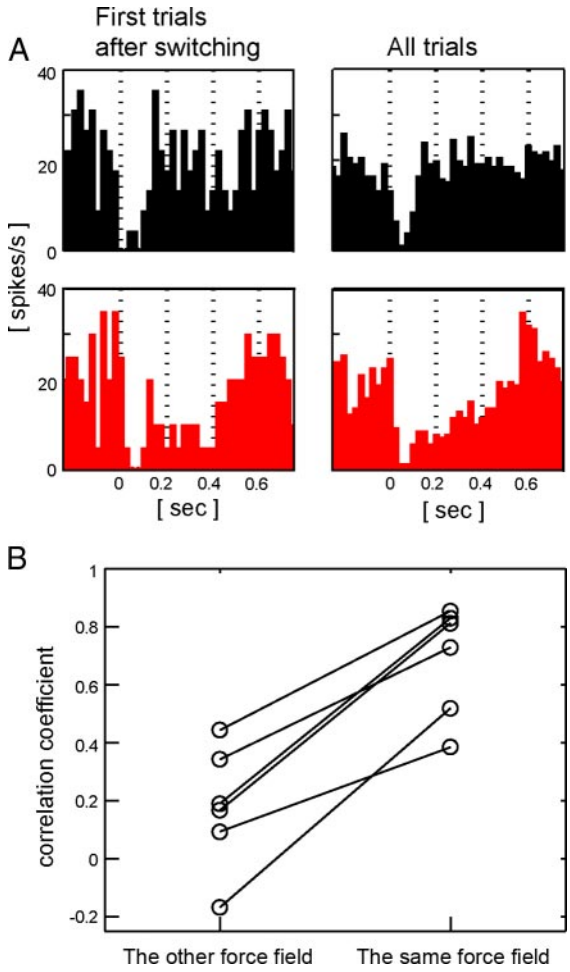

FIG. 10. Instantaneous switching of simple spike activity after training. *A*: SS activities in the 1st trials after switching (*left*) and activities averaged over all trials (*right*). The data were obtained from a Purkinje cell of *monkey M* during flexion under the resistive (*top*) and assistive (*bottom*) force fields. The histograms are aligned on movement onset. Bin width is 25 ms. *B*: correlation of the SS activities in the first trials with those in the same force field (*right*) and those in the other (preceding) force field (*left*). Note the larger correlation with activity in the same force field than that with activity in the preceding force field.

significant in all combinations of muscles and Purkinje cells ($P < 0.0001$) although the determination coefficient (r^2) was 0.17 on average and 0.52 at the largest (Fig. 11*B*).

When the velocity profiles were reconstructed from SS activity of single Purkinje-cells, the distribution of the estimated time lag distributed with the mode of −30 and 0 ms (Fig. 11*C*). Estimated time lags were negative in around half of Purkinje cells (60% in *monkey M,* 48% in *monkey P*). The determination coefficient was 0.18 on average and 0.71 at the largest.

The results show that SS activity of individual Purkinje cell could explain a part of movement kinematics as well as a part of movement dynamics. To see whether Purkinje cells with SS activity that led movement kinematics were different from those that led movement dynamics, we thresholded the determination coefficients at 0.1 ($P < 10^{-5}$, uncorrected). Of the 60 Purkinje cells from the two monkeys, 49 (82%) led EMG activity of either biceps or triceps muscle (dynamics group) and 27 (45%) led velocity profiles (kinematics group) with an overlap of 16 (27%) between the two groups (Fig. 12*A*). The two groups of neurons seemed to overlap in the recorded area (Fig. 12*B*).

DISCUSSION

In the present study, we trained monkeys to carry out arm movements with almost identical velocity profiles (kinematics), but with distinct muscle activities (dynamics), by applying two distinctively different force fields. We showed that SS activity recorded from Purkinje cells in the intermediate part of the cerebellum (lobules V–VI) differed depending on the type of force field. We confirmed this quantitatively by showing that SS activities encoded much larger mutual information with the type of force field than that with the residual difference in the velocity profiles. The disparity in SS activities due to the difference in force fields appeared ~40 ms prior to the appearance of the disparity in EMG activities. We further found that SS activity of many Purkinje cells correlated with EMG activity with a lead of ~80 ms. These results suggest that SS activity of at least a group of Purkinje cells in the intermediate part of cerebellar lobules V–VI encodes movement dynamics that might be transformed into EMG activities with a latency of 40–80 ms.

Dynamics or kinematics?

Several previous studies have reported that SS activity of Purkinje cells in and around cerebellar lobule V correlated with movement kinematics (Coltz et al. 1999, 2000; Fortier et al. 1989; Fu et al. 1997; Mano and Yamamoto 1980). These studies do not necessarily contradict our finding even if we assume that SSs encode movement dynamics because movement kinematics are often correlated with movement dynamics

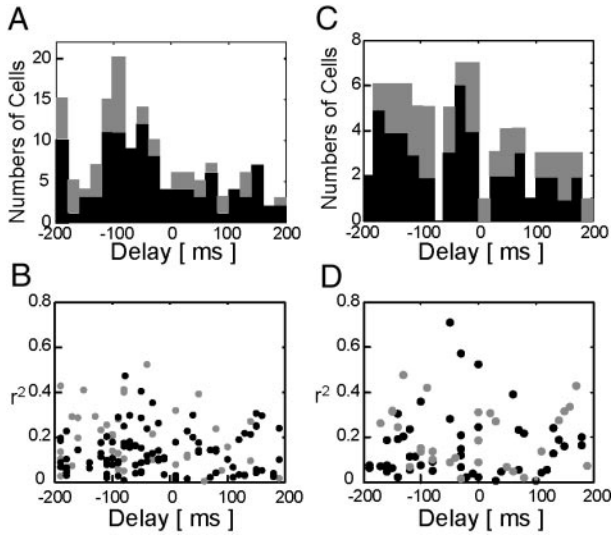

FIG. 11. *A*: distribution of estimated time delays (*d* in *Eq. 4*) between EMG activity and the SS activity. EMG activities of each muscle were approximated by the SS firing rate recorded from each single Purkinje cell. Negative time delays (mode = −80 ms) show that SS activity led that of EMG. ■ and ▨, data from *monkeys M* and *P,* respectively. *B*: determination coefficients (r^2) of single Purkinje cells plotted against the estimated time delays. ● and ◍, data from *monkeys M* and *P,* respectively. *C*: distribution of estimated time delays between velocity and the SS activity. *D*: determination coefficients of single Purkinje cells plotted against the estimated time delays.

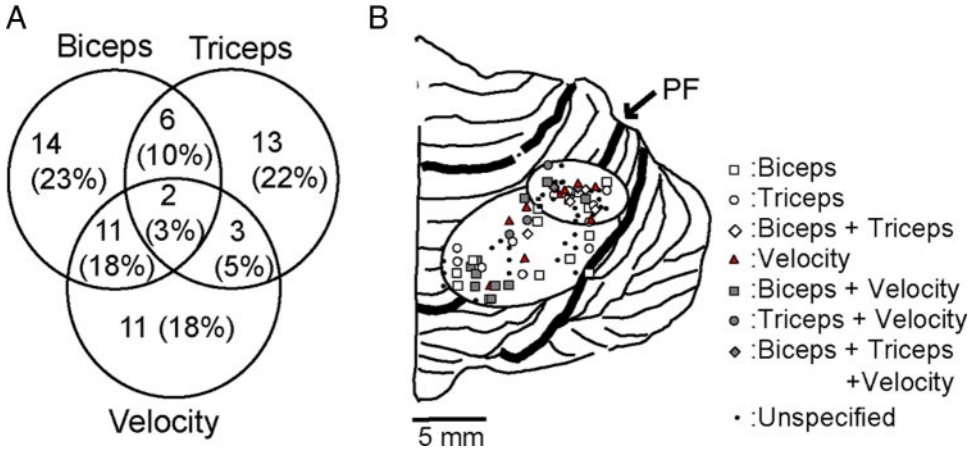

FIG. 12. Distributions of Purkinje cells with SS activity related to muscle activities (dynamics) and velocity profiles (kinematics). *A*: Venn diagram of 3 groups of neurons: those with SS activity that correlated with EMG of biceps, EMG of triceps, and velocity profiles. Determination coefficients (r^2) were thresholded at 0.1. Percentage was calculated against 60 Purkinje cells that were analyzed. *B*: distribution of each group on a dorsal view of the cerebellar cortex. Each symbol represents each subgroup as indicated in the diagram in *A*. In general, open symbols and red symbols show correlation with EMG and velocity, respectively. Neurons in the overlaps are represented by gray symbols.

(Todorov 2000). To conclude whether SSs are encoding movement kinematics or dynamics, it is critically important to remove the correlation between these parameters. We removed the correlation by training animals to carry out arm movements with almost identical kinematics, but with distinct dynamics, and showed that SS activity of some Purkinje cells in the intermediate part of cerebellar lobules V–VI encodes movement dynamics. However, this does not preclude the possibility that some Purkinje cells in the same area encode movement kinematics. By applying linear regression analysis, we indeed found that SS activity of some Purkinje cells led movement kinematics, whereas others led movement dynamics. This may suggest that both dynamics and kinematics are encoded by SS activity of Purkinje cells in the intermediate part of cerebellar lobules V–VI and that there are two groups of neurons representing dynamics or kinematics but with some overlap between the two. Outputs from the two groups of neurons may project to corresponding groups of neurons in the primary motor cortex (Kelly and Strick 2003), one encoding movement dynamics and the other encoding movement kinematics (Evarts 1968; Kakei et al. 1999; Kalaska et al. 1989; Scott and Kalaska 1997; Sergio and Kalaska 1997, 1998). The best way to confirm the existence of Purkinje cells that encode movement kinematics, however, is to carry out complementary experiments in which animals perform arm movements with almost identical dynamics but with distinct kinematics.

Coltz et al. (1999) reported that SSs in the intermediate and lateral regions of lobules V-VI correlated with the direction and speed of slow arm movements. They further emphasized that in most EMG recordings, EMGs in the slow arm movements did not correlate with the mean movement speed. From the results, they suggested that SSs encoded movement kinematics but not dynamics. However, 5 of 12 muscles (acromiodeltoid, biceps, flexor carpi radialis, spinodeltoid, and triceps) in their study did show speed-related modulation (Coltz et al. 1999). In addition, 45% (61 or 135) of EMG recordings were significantly fitted by a model that incorporated both movement speed and direction (Coltz et al. 1999). The percentage (45%) may be "far smaller" than the percentage of significant fit to velocity in SS discharge of Purkinje cells (70%, 92 of 132) but may not be so small as to exclude any possibility that the EMG activity of some critical muscles correlated with movement kinematics. It is worth noting again that encoding of kinematics would be verified by carrying out experiments in which animals perform task movements with identical dynamics but with distinct kinematics.

Recently Liu et al. (2003) dissociated a correlation between cursor and arm movements using a task in which a cursor on a monitor moved in the same or opposite direction to that of arm movements. They found two different groups of neurons in the lateral regions in and around cerebellar lobule V. The activities of neurons in one group correlated with the movement direction of the visual cursor movements (cursor-related neurons) and the activities of another group of neurons correlated with the direction of arm movements (task-related neurons). It is possible that task-related neurons encoded movement dynamics. Cursor-related neurons, on the other hand, might have encoded movement kinematics rather than dynamics. However, Liu et al. (2003) did not find significant trial-by-trial correlation between peak movement velocity and neuronal modulation levels for all cursor-related cells. Thus these cursor-related neurons may consist of a group of neurons that are different from those encoding arm movements per se. It is worth noting that most of these cursor-related neurons were found in the lateral part of the cerebellum (Liu et al. 2003) from which we did not record many neurons.

Mano and Yamamoto (1980) examined SS activity of Purkinje cells in the intermediate and lateral parts of lobules IV–VI during wrist flexion and extension. They reported that SS activity was often nonreciprocal in that the activity was increased (or decreased) in both directions in marked contrast to EMG activities of wrist-related muscles that were modulated reciprocally. The results of Mano and Yamamoto (1980) agree with those of the present study. For example, a Purkinje cell in Fig. 5*C* showed a nonreciprocal decrease during both flexion and extension under the resistive force field (black curves). However, the same neuron showed different patterns of activity under the assistive force field (red curves). Nonreciprocal modulation in one condition does not preclude the possibility that the neuron encodes movement dynamics.

Our finding that SS activity encodes movement dynamics during elbow movements agrees with previous findings in ocular and wrist movements (Gilbert and Thach 1977; Gomi et al. 1998; Shidara et al. 1993). Shidara et al. (1993) and Gomi et al. (1998) showed that SS activity recorded from Purkinje cells in the ventral paraflocculus can be reconstructed by an inverse dynamics representation of the eye movement. They concluded that these Purkinje cells primarily encode dynamic

components of the motor command. Gilbert and Thach (1977) examined SS activity during a wrist-movement task in which monkeys were required to keep a neutral position of a manipulandum by flexing or extending the wrist against a load perturbation. When the magnitude of the load was altered, the monkeys took ~12–100 trials with the novel load before performing as regularly as previously. After the adaptation to the new load, wrist movements became similar to those in the preadaptation period, but SS discharge was altered. The results suggest that SS activity reflects load (dynamics) rather than the kinematics of the wrist movement though the kinematics of movements were not examined in detail. We verified SS encoding of dynamics in elbow joint movements by assuring that the velocity profiles were almost identical under distinctively different force fields.

It is worth noting in addition that it took 12–100 trials for the monkeys to adapt to the new load in Gilbert and Thach (1977), and it took as many trials for the SSs to achieve a postadaptation firing level. On the other hand, in the present study, the monkeys were able to switch between the two motor skills from the first trial after the force field was switched from one to the other. Accordingly SS activity was also switched from the first trial (Fig. 10). The difference might be due to the presence of the color cue in the present study and the absence of such a salient cue in Gilbert and Thach (1977). Contextual cues like distinct background colors may be essential or at least beneficial for the acquisition and switching of two independent motor skills under distinct force fields (Wada et al. 2003).

Transformation from SS to EMG

It has been reported that SS activity of many Purkinje cells in lobules V–VI led movement onsets of the arm, wrist, and fingers (Coltz et al. 1999; Fortier et al. 1989; Fu et al. 1997; Liu et al. 2003; Mano and Yamamoto 1980; Smith and Bourbonnais 1981; Thach 1968, 1970). When the onset of SS activity was compared with the onset of EMG activity, the lead time was ~20–80 ms on average (Smith and Bourbonnais 1981; Thach 1970) among those neurons that led EMG onsets.

In the present study, the onset of modulation in SS activities led the onset of EMG modulation by 20–40 ms (Fig. 9). Reconstruction of the EMG activities from SS activities in single Purkinje cells had a delay of ~80 ms on average (Fig. 11). These values (20–80 ms) were in good agreement with the mean leading time of SS activity in the previous studies (Smith and Bourbonnais 1981; Thach 1970).

Miller and his colleagues reconstructed the temporal patterns of EMGs from neural activities in the primary motor cortex (Morrow and Miller 2003) and those in the red nucleus (Miller and Sinkjaer 1998) by using a linear regression model that was similar to the model in the present study. The estimated delays from the neural activities to EMG activity were ~50 ms in the primary motor cortex as well as in the red nucleus. These values were comparable to the delay from the Purkinje cell activity to EMG (~80 ms) estimated in the present study. This is reasonable because the intermediate part of the cerebellar lobules IV–VI has tri-synaptic connections to and from the primary motor cortex (Kelly and Strick 2003) and disynaptic projections to neurons in the red nucleus via the deep cerebellar nuclei.

Miller and his colleagues suggested that activity of multiple neurons in the primary motor cortex (Morrow and Miller 2003) and the red nucleus (Miller and Sinkjaer 1998) are summed into the muscle activity in the spinal cord. Because Purkinje cells are located upstream of these structures, it is not surprising that SS activity of a single Purkinje cell was not sufficient to reconstruct EMG activity (Fig. 11*B*). From the results of the present study and those of Miller and colleagues (Miller and Sinkjaer 1998; Morrow and Miller 2003), we suggest the possibility that activities of a group of Purkinje cells in the intermediate part of the cerebellum are transformed almost linearly into activities in the red nucleus and those in the primary motor cortex then summed into the muscle activity in the spinal cord.

Cerebellum and multiple motor skills

Our animals were able to switch their muscle activities and produce almost identical velocity patterns from the first trial after the force field was switched from one to the other (Fig. 4). This instantaneous switching was in agreement with previous studies in humans (Wada et al. 2003) and a monkey (Krouchev and Kalaska 2003) that used the same apparatus as in the present study. This type of instantaneous switching of motor skills under different force fields has been reported in experiments with salient (large field) color cues (Krouchev and Kalaska 2003; Osu et al. 2004; Wada et al. 2003) but not in studies without salient cues (Li et al. 2001; Padoa-Schioppa et al. 2002). Presentation of salient color cues (black and red) and extensive training in the present study must have contributed to the acquisition of instantaneous switching between two motor skills.

In explaining such ability to switch between multiple motor skills, it is hypothesized that the CNS learns and maintains multiple internal models and switches between them (Haruno et al. 2001; Kawato 1999; Osu et al. 2004; Wolpert and Kawato 1998). The present results agree with the theoretical framework that instantaneous switching is achieved by a responsibility predictor, which computes the responsibility signal, the gating signal, from only contextual information and can predictively switch between different internal models (Kawato 1999; Wolpert and Kawato 1998).

Imaging studies have suggested that the cerebellum is a candidate that acquires, maintains, and switches among multiple internal models (Imamizu et al. 2000, 2003, 2004). In theory, an inverse dynamics model that provides movement dynamics and also a forward kinematics model that outputs movement kinematics are acquired in pairs for controlling each motor skill (Haruno et al. 2001; Imamizu et al. 2004; Wolpert and Kawato 1998). Existence of two groups of neurons, representing dynamics or kinematics, suggests that SS activities in the intermediate part of cerebellar lobule V–VI constitute outputs of multiple internal models that provide different movement dynamics as well as kinematics. We also found that there are single Purkinje cells the SS activity of which fairly well explained the variance of EMG activity under the two force fields. The results suggest that some Purkinje cells represent correct motor commands that are utilized for movement control under different force fields. This agrees with one of two possibilities proposed in a previous imaging study (Fig. 8*B* of Imamizu et al. 2004); that is, the weighting from many

inverse-model outputs for computing the final motor command is carried out already in the cerebellum rather than outside the cerebellum.

ACKNOWLEDGMENTS

We are very grateful to R. N. Lemon for technical advice on implantation of the EMG patches and D. S. Hoffman for improving the manuscript. We thank T. Takada, T. Takasu, M. Uchiyama, and A. Kameyama, for technical assistance and T. Tanaka and S. Inoue for secretarial help.

GRANTS

This work was supported by grants from Human Frontier Science Program to S. Kitazawa and M. Kawato and a Grant-in-Aid for Scientific Research on Priority Areas-System study on higher-order brain functions-from MEXT (17022033) to S. Kitazawa. K. Yamamoto was supported by a Domestic Research Fellowship Foundation of Japan Science and Technology and a Domestic Research Fellowship Foundation of Japan Society for the Promotion of Science.

REFERENCES

Coltz JD, Johnson MT, Ebner TJ. Cerebellar Purkinje cell simple spike discharge encodes movement velocity in primates during visuomotor arm tracking. *J Neurosci* 19: 1782–1803, 1999.

Coltz JD, Johnson MT, Ebner TJ. Population code for tracking velocity based on cerebellar Purkinje cell simple spike firing in monkeys. *Neurosci Lett* 296: 1–4, 2000.

Evarts EV. Relation of pyramidal tract activity to force exerted during voluntary movement. *J Neurophysiol* 31: 14–27, 1968.

Fortier PA, Kalaska JF, Smith AM. Cerebellar neuronal activity related to whole-arm reaching movements in the monkey. *J Neurophysiol* 62: 198–211, 1989.

Fu QG, Flament D, Coltz JD, Ebner TJ. Relationship of cerebellar Purkinje cell simple spike discharge to movement kinematics in the monkey. *J Neurophysiol* 78: 478–491, 1997.

Gilbert PF, Thach WT. Purkinje cell activity during motor learning. *Brain Res* 128: 309–328, 1977.

Gomi H, Shidara M, Takemura A, Inoue Y, Kawano K, Kawato M. Temporal firing patterns of Purkinje cells in the cerebellar ventral paraflocculus during ocular following responses in monkeys. I. Simple spikes. *J Neurophysiol* 80: 818–831, 1998.

Haruno M, Wolpert DM, Kawato M. Mosaic model for sensorimotor learning and control. *Neural Comput* 13: 2201–2220, 2001.

Imamizu H, Kuroda T, Miyauchi S, Yoshioka T, Kawato M. Modular organization of internal models of tools in the human cerebellum. *Proc Natl Acad Sci USA* 100: 5461–5466, 2003.

Imamizu H, Kuroda T, Yoshioka T, Kawato M. Functional magnetic resonance imaging examination of two modular architectures for switching multiple internal models. *J Neurosci* 24: 1173–1181, 2004.

Imamizu H, Miyauchi S, Tamada T, Sasaki Y, Takino R, Putz B, Yoshioka T, Kawato M. Human cerebellar activity reflecting an acquired internal model of a new tool. *Nature* 403: 192–195, 2000.

Kakei S, Hoffman DS, Strick PL. Muscle and movement representations in the primary motor cortex. *Science* 285: 2136–2139, 1999.

Kalaska JF, Cohen DA, Hyde ML, Prud'homme M. A comparison of movement direction-related versus load direction-related activity in primate motor cortex, using a two-dimensional reaching task. *J Neurosci* 9: 2080–2102, 1989.

Kawano K. Ocular tracking: behavior and neurophysiology. *Curr Opin Neurobiol* 9: 467–473, 1999.

Kawato M. Internal models for motor control and trajectory planning. *Curr Opin Neurobiol* 9: 718–727, 1999.

Kawato M, Gomi H. A computational model of four regions of the cerebellum based on feedback-error learning. *Biol Cybern* 68: 95–103, 1992.

Kelly RM, Strick PL. Cerebellar loops with motor cortex and prefrontal cortex of a nonhuman primate. *J Neurosci* 23: 8432–8444, 2003.

Kitazawa S, Kimura T, Yin PB. Cerebellar complex spikes encode both destinations and errors in arm movements. *Nature* 392: 494–497, 1998.

Krouchev NI, Kalaska JF. Context-dependent anticipation of different task dynamics: rapid recall of appropriate motor skills using visual cues. *J Neurophysiol* 89: 1165–1175, 2003.

Li CS, Padoa-Schioppa C, Bizzi E. Neuronal correlates of motor performance and motor learning in the primary motor cortex of monkeys adapting to an external force field. *Neuron* 30: 593–607, 2001.

Liu X, Robertson E, Miall RC. Neuronal activity related to the visual representation of arm movements in the lateral cerebellar cortex. *J Neurophysiol* 89: 1223–1237, 2003.

Mano N, Yamamoto K. Simple-spike activity of cerebellar Purkinje cells related to visually guided wrist tracking movement in the monkey. *J Neurophysiol* 43: 713–728, 1980.

Miles FA, Fuller JH, Braitman DJ, Dow BM. Long-term adaptive changes in primate vestibuloocular reflex. III. Electrophysiological observations in flocculus of normal monkeys. *J Neurophysiol* 43: 1437–1476, 1980.

Miller LE, Sinkjaer T. Primate red nucleus discharge encodes the dynamics of limb muscle activity. *J Neurophysiol* 80: 59–70, 1998.

Miller LE, van Kan PL, Sinkjaer T, Andersen T, Harris GD, Houk JC. Correlation of primate red nucleus discharge with muscle activity during free-form arm movements. *J Physiol* 469: 213–243, 1993.

Morrow MM, Miller LE. Prediction of muscle activity by populations of sequentially recorded primary motor cortex neurons. *J Neurophysiol* 89: 2279–2288, 2003.

Osu R, Hirai S, Yoshioka T, Kawato M. Random presentation enables subjects to adapt to two opposing forces on the hand. *Nat Neurosci* 7: 111–112, 2004.

Padoa-Schioppa C, Li CS, Bizzi E. Neuronal correlates of kinematics-to-dynamics transformation in the supplementary motor area. *Neuron* 36: 751–765, 2002.

Scott SH, Kalaska JF. Reaching movements with similar hand paths but different arm orientations. I. Activity of individual cells in motor cortex. *J Neurophysiol* 77: 826–852, 1997.

Sergio LE, Kalaska JF. Systematic changes in directional tuning of motor cortex cell activity with hand location in the workspace during generation of static isometric forces in constant spatial directions. *J Neurophysiol* 78: 1170–1174, 1997.

Sergio LE, Kalaska JF. Changes in the temporal pattern of primary motor cortex activity in a directional isometric force versus limb movement task. *J Neurophysiol* 80: 1577–1583, 1998.

Shidara M, Kawano K, Gomi H, Kawato M. Inverse-dynamics model eye movement control by Purkinje cells in the cerebellum. *Nature* 365: 50–52, 1993.

Smith AM, Bourbonnais D. Neuronal activity in cerebellar cortex related to control of prehensile force. *J Neurophysiol* 45: 286–303, 1981.

Thach WT. Discharge of Purkinje and cerebellar nuclear neurons during rapidly alternating arm movements in the monkey. *J Neurophysiol* 31: 785–797, 1968.

Thach WT. Discharge of cerebellar neurons related to two maintained postures and two prompt movements. II. Purkinje cell output and input. *J Neurophysiol* 33: 537–547, 1970.

Todorov E. Direct cortical control of muscle activation in voluntary arm movements: a model. *Nat Neurosci* 3: 391–398, 2000.

Wada Y, Kawabata Y, Kotosaka S, Yamamoto K, Kitazawa S, Kawato M. Acquisition and contextual switching of multiple internal models for different viscous force fields. *Neurosci Res* 46: 319–331, 2003.

Wolpert DM, Kawato M. Multiple paired forward and inverse models for motor control. *Neural Netw* 11: 1317–1329, 1998.

Yamamoto K, Kawato M, Kotosaka S, Kitazawa S. Purkinje-cell activity during arm movements under different viscous fields. *Soc Neurosci Abstr* Program No. J-7, 2002a.

Yamamoto K, Kawato M, Kotosaka S, and Kitazawa S. Reconstruction of EMG activity from linear summation of Purkinje-cell activity during arm movements in the monkey. *Jpn J Physiol Suppl* 52: S159, 2002b.

Yamamoto K, Kobayashi Y, Takemura A, Kawano K, Kawato M. Computational studies on acquisition and adaptation of ocular following responses based on cerebellar synaptic plasticity. *J Neurophysiol* 87: 1554–1571, 2002c.

Yamamoto K, Kotosaka S, Kawato M, Kitazawa S. An animal model of instantaneous switching of motor skills. *Neurosci Res Suppl* 24: 154, 2000.